

determined by capillary gas chromatography on a 25-m methylsilicone column in a Hewlett Packard Model 3890 gas chromatograph with use of both N,P-thermionic and flame ionization detectors. An authentic sample of tetraphenylhydrazine was thermolyzed in benzene- d_6 at 80 °C and used to confirm the identity of the products obtained.

Amide thermolysis in the presence of 9,10-dihydroanthracene was carried out in benzene- d_6 at 65 °C by the same techniques. Both amide and DHA were added to the NMR tubes and solvent was added. Concentrations were determined by sample height. Concentration vs. time data were acquired automatically with Nicolet KINET software and was analyzed with RS1 software operating on a VAX 11/780 system. Figure 3 shows the loss of amide plots obtained, while the rate dependence on dihydroanthracene is shown on Figure 4. Products were identified by spiking product solutions with authentic samples of $\text{Cp}^*(\text{PMe}_3)_2\text{RuH}$, HNPh_2 , and anthracene. Both GC and NMR methods were used.

When trimethylphosphine was added to a solution of amide and 9,10-dihydroanthracene in benzene- d_6 ($[\text{Cp}^*(\text{PMe}_3)_2\text{RuNPh}_2] = 0.052$

M; $[\text{PMe}_3] = 0.20$ M; $[9,10\text{-DHA}] = 0.80$ M) thermolysis at 60 °C demonstrated the loss of amide to be faster than in the absence of phosphine. Only ca. 60% of the amide was converted to hydride in this case (the other products were not identified), and during the thermolysis ^{31}P CIDNP signals were noted.

Acknowledgment. The technical assistance of Martin A. Cushing, Jr., Joseph P. Foster, Jr., and Barry D. Johnson is gratefully acknowledged. We also appreciate the efforts of Mr. E. A. Conaway in obtaining some of the T_s data needed for these studies. We thank Drs. David M. Golden and Gregory P. Smith of the Chemical Kinetics research group at SRI International and Professor Robert H. Grubbs at CIT for valuable discussions. This work was supported by the DuPont Company and, in part, by the National Science Foundation (Grant CHE-8303735), which is gratefully acknowledged.

A Kinetic Study of the Epoxidation of 2,3-Dimethyl-2-butene by *tert*-Butyl Hydroperoxide Catalyzed by Imidazole Ligated (*meso*-Tetraphenylporphinato)manganese(III)

P. N. Balasubramanian, Ashoke Sinha, and Thomas C. Bruice*

Contribution from the Department of Chemistry, University of California at Santa Barbara, Santa Barbara, California 93106. Received May 12, 1986

Abstract: A kinetic study of the epoxidation of 2,3-dimethyl-2-butene (TME) by *t*-BuOOH in the presence of (*meso*-tetraphenylporphinato)manganese(III) chloride ($(\text{TPP})\text{Mn}^{\text{III}}\text{Cl}$) and imidazole (ImH) has been carried out (30 °C, CH_2Cl_2 solvent). The rates of decrease in $[t\text{-BuOOH}]$ and increase in $[\text{epoxide}]$ have been determined as a function of the initial concentrations of $[t\text{-BuOOH}]$, $[\text{TME}]$, $[\text{ImH}]$, and $[(\text{TPP})\text{Mn}^{\text{III}}\text{Cl}]$. As found previously, ImH ligation is required for the reaction of the manganese(III) porphyrin with *t*-BuOOH and thus for the epoxidation of TME. Under the condition of $[t\text{-BuOOH}]_0$, $[\text{TME}]_0$, and $[\text{ImH}]_0 \gg [(\text{TPP})\text{Mn}^{\text{III}}\text{Cl}]_0$, it is found that the rate for disappearance of *t*-BuOOH is always more than twofold greater than is the rate of epoxide formation regardless of the ratios of $[t\text{-BuOOH}]$, $[\text{ImH}]$, and $[\text{TME}]$. This requires that in addition to an ImH ligated higher valent manganese oxo porphyrin there is the formation of an additional intermediate species capable of transferring oxygen. This must be so, because the total concentration of $(\text{TPP})\text{Mn}^{\text{III}}\text{Cl}$ is not sufficient to store the oxygen equivalents. Other pertinent observations are as follows: (i) Disappearance of *t*-BuOOH follows the first-order rate law in the absence of TME while in the presence of TME its disappearance follows two sequential first-order processes; (ii) formation of epoxide is always first-order; (iii) the maximum yield of epoxide is but ~60%; (iv) the % yield of epoxide increases and then decreases with increase in $[\text{ImH}]_0$; and (v) there is formation of a small percentage of di-*tert*-butyl peroxide ($(t\text{-BuO})_2$). A proposed reaction sequence which is competent in accounting for these observations is presented in Scheme I. The equilibrium constants for ligation of ImH with manganese(III) porphyrin and the rate constants for oxygen transfer from *t*-BuOOH to both $(\text{TPP})\text{Mn}^{\text{III}}(\text{ImH})\text{Cl}$ and $(\text{TPP})\text{Mn}^{\text{III}}(\text{ImH})_2$ were determined individually while the other constants of Scheme I were obtained as the best minimal values by computer simulation of the time dependence for the disappearance of *t*-BuOOH and appearance of epoxide and $(t\text{-BuO})_2$.

The impetus to study oxygen atom transfer oxidations with iron(III) and manganese(III) porphyrins has been to gain basic chemical knowledge essential to an understanding of the mechanisms of the peroxidase and cytochrome P-450 enzymes and also to provide new synthetic approaches to such reactions as oxygen insertion into C-H bonds and selective epoxidations.^{1,2} (*meso*-Tetraphenylporphinato)manganese(III) chloride ($(\text{TPP})\text{Mn}^{\text{III}}\text{Cl}$) is a good catalyst for oxidations with iodosylbenzene and percarboxylic acids but not reactive with alkyl hydroperoxides³ as such. Ligation by imidazoles⁴ and pyridines⁵ greatly enhances

the reactivity of manganese(III) porphyrin salts with alkyl hydroperoxides and hypochlorite. Mansuy et al.^{4c} reported that addition of imidazole increases the yield of epoxide when using cumyl hydroperoxide as an oxidant with a manganese(III) porphyrin. In quantitative studies, we have shown that exchange of Cl^- ligand for imidazole (ImH) dramatically increases the rate constants for oxygen transfer to manganese(III) porphyrin from both percarboxylic acids and alkyl hydroperoxides.⁶ The former reaction involves rate-determining heterolytic O-O bond scission and the latter most likely rate-determining homolytic bond scission.

(1) (a) Morrison, M.; Schonbaum, G. R. *Annu. Rev. Biochem.* **1976**, *45*, 861. (b) Dunford, H. B.; Stillman, J. S. *Coord. Chem. Rev.* **1976**, *19*, 187. (c) Coon, M. J.; White, R. E. In *Metal Ion Activation of Dioxigen*; Spiro, T. G., Ed.; John Wiley and Sons: New York, 1980; pp 73-123. (d) Omura, T. In *Cytochrome P-450*; Sato, R., Omura, T., Eds.; Kodansha Ltd.: Tokyo, 1978; pp 138-163. (e) Ullrich, V. *J. Mol. Catal.* **1980**, *7*, 159.

(2) Gelb, M. H.; Toscano, W. A., Jr.; Sligar, S. G. *Proc. Natl. Acad. Sci. U.S.A.* **1982**, *79*, 5758.

(3) (a) Yuan, L.-C.; Bruice, T. C. *Inorg. Chem.* **1985**, *24*, 986. (b) Mansuy, D.; Bartoli, J.-F.; Momenteau, M. *Tetrahedron Lett.* **1982**, *23*, 2781. (c) Mansuy, D.; Bartoli, J.-F.; Chottard, J.-C.; Lange, M. *Angew. Chem., Int. Ed. Engl.* **1980**, *19*, 909. (d) Hill, C. L.; Smegal, J. A.; Henly, T. J. *J. Org. Chem.* **1983**, *48*, 3277.

(4) (a) Collman, J. P.; Brauman, J. I.; Meunier, B.; Hayashi, T.; Kodadek, T.; Raybuck, S. A. *J. Am. Chem. Soc.* **1985**, *107*, 2000. (b) Collman, J. P.; Brauman, J. I.; Meunier, B.; Raybuck, S. A.; Kodadek, T. *Proc. Natl. Acad. Sci. U.S.A.* **1984**, *81*, 3245. (c) Mansuy, D.; Battioni, P.; Renaud, J.-P. *J. Chem. Soc., Chem. Commun.* **1984**, 1255.

(5) (a) Guilmet, E.; Meunier, B. *Nouv. J. Chim.* **1982**, *6*, 511. (b) Meunier, B.; Guilmet, E.; Carvalho, M.-E. D.; Poilblanc, R. *J. Am. Chem. Soc.* **1984**, *106*, 6668. (c) Collman, J. P.; Kodadek, T.; Raybuck, S. A.; Meunier, B.; *Proc. Natl. Acad. Sci. U.S.A.* **1983**, *80*, 7039. (d) Guilmet, E.; Meunier, B. *J. Mol. Catal.* **1984**, *23*, 115. (e) Van der Made, A. W.; Nolte, R. J. M. *J. Mol. Catal.* **1984**, *26*, 333. (f) Razenberg, J. A. S. J.; Nolte, R. J. M.; Drenth, W. *Tetrahedron Lett.* **1984**, *25*, 789.

(6) Yuan, L.-C.; Bruice, T. C. *J. Am. Chem. Soc.* **1986**, *108*, 1643.

Collman and collaborators^{4a,b} have provided evidence for the formation of an intermediate in the epoxidation of alkenes by hypochlorite when catalyzed by nitrogen base ligated manganese(III) porphyrins. In the present investigation the time courses for disappearance of the oxygen donor (*t*-BuOOH) in the absence and presence of alkene (2,3-dimethyl-2-butene, TME) as well as formation of TME epoxide (TMEO) have been followed in the presence of imidazole and (tetraphenylporphinato)manganese(III) chloride. Epoxide formation is slower, under all the experimental conditions employed, than is *t*-BuOOH disappearance. This observation is shown to involve the accumulation of a nonporphyrin oxygen carrier species.

Experimental Section

Materials. Dichloromethane was purchased from Burdick and Jackson Laboratories, Inc. (99.9%, "distilled in glass" grade), and this was passed through an alumina column before use. Tetramethylethylene (TME) was bought from Aldrich Chemical Laboratories (99% pure). By GC analysis the TME was shown to be of 98% purity. Traces of tetramethylethylene oxide (TMEO) were removed by stirring over P_2O_5 , and distillation over metallic sodium under nitrogen followed by passing through an alumina column which had previously been baked at 110 °C. TMEO was prepared by a standard procedure⁷ from TME and *m*-chloroperbenzoic acid in dichloromethane and finally purified by distillation. (*meso*-Tetraphenylporphinato)manganese(III) chloride ((TPP)- $Mn^{III}Cl$) was prepared and purified according to a literature procedure.⁸ *tert*-Butylhydroperoxide (*t*-BuOOH) (anhydrous, 3.0 M solution in toluene) was purchased from Aldrich and used without further purification. Di-*tert*-butylperoxide (EM Science) was used as received. The concentration of *t*-BuOOH was determined by iodometric titration.⁹ 2,2-Diphenyl-1-picrylhydrazylhydrate radical (DPP*) (95%) was available from Aldrich. Sodium dithionite reduction of DPP* afforded 2,2-diphenyl-1-picrylhydrazine (DPPH), which was recrystallized twice from $CHCl_3$ /EtOH (2:3).¹⁰ Imidazole (ImH) (Aldrich) was twice recrystallized from benzene.

Instrumentation. Ultraviolet and visible absorption spectra and, also, the spectral kinetic data were recorded on a Cary 118C or Perkin-Elmer 553 fast-scanning spectrophotometer. GC analysis was carried out with a Varian 3700 Model chromatograph equipped with Hewlett-Packard 3392A Model integrator by using a 20-m capillary column (Varian 50QC2/BPI, WCOT, Vit. Silica). Pseudo-first-order rate constants were determined from plots of kinetic data by use of a Hewlett Packard 9825A computer equipped with a 9864A digitizer and a 9862A calculator plotter. All experiments were performed under nitrogen atmosphere in a glovebox. Kinetic simulations were performed on a DEC VAX 11-750 employing software designed about Gear Integrators.

Kinetic studies were carried out at 30 °C in dichloromethane under nitrogen atmosphere. In a typical run a 456- μ L aliquot of dichloromethane containing appropriate amounts of (TPP)- $Mn^{III}Cl$, imidazole, TME, and/or DPPH was injected into a 1-mL sealed Wheaton serum bottle containing a nitrogen atmosphere. This was placed inside a 10-mL vial containing dichloromethane and closed with a rubber septum. The principle behind the technique was to reduce the loss of dichloromethane from the reaction vial by saturating the outer envelope with dichloromethane from the outer vial. The whole system was prepared inside a glovebox and then taken out to be placed in a constant temperature bath at 30 °C. A freshly prepared dichloromethane solution of *t*-BuOOH (44.0 μ L) was injected to start the reaction, and its progress was followed by frequently withdrawing 0.5 μ L of the sample for injection into the GC. In quantitating the peak areas of TMEO and *t*-BuOOH, standard plots of the authentic sample were constructed from the GC readings under identical conditions of column temperature and the flow rate of the inlet gas. The toluene present in the solution (being the solvent for the *tert*-butylhydroperoxide) served as an internal standard for injection volumes.

Results

The kinetics (CH_2Cl_2 solvent, 30 °C, N_2 atmosphere) for disappearance of *t*-BuOOH (8.2×10^{-3} – 1.6×10^{-1} M) and appearance of TMEO from epoxidation of 2,3-dimethyl-2-butene

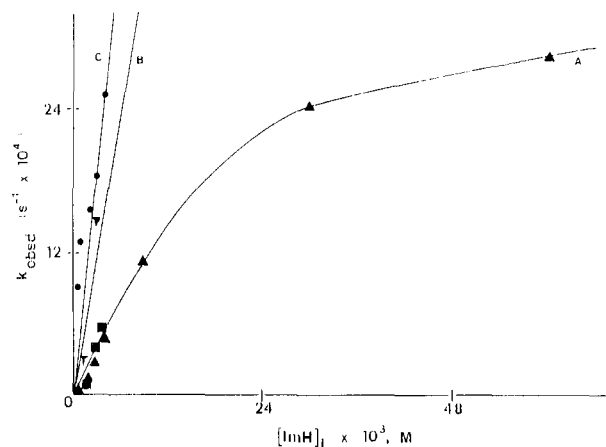


Figure 1. A plot of the pseudo-first-order rate constant (k_{obs}) vs. $[ImH]_i$ at constant $[(TPP)Mn^{III}Cl]_i = 6.0 \times 10^{-4}$ M, $[t-BuOOH]_i = 8.2 \times 10^{-3}$ M, and $[TME]_i = 0.40$ M. Line A correlates both the rate constant (k_e) for the formation of TMEO (\blacktriangle) and the rate constant (k_h) for the decomposition of *t*-BuOOH (\blacktriangledown); line B correlates the observed rate constants for the initial and rapid component for the biphasic decomposition of *t*-BuOOH (\blacktriangledown) (initial 15–20% of reaction). Line C pertains to the rate constant (k_h') for the decomposition of *t*-BuOOH when TME is not included (\bullet).

(TME = 2×10^{-2} – 7×10^{-1} M) were monitored in the presence (2×10^{-3} – 6×10^{-2} M) and absence of imidazole employing (*meso*-tetraphenylporphinato)manganese(III) chloride ((TPP)- $Mn^{III}Cl$) (1.2×10^{-4} – 6×10^{-4} M) as catalyst. The decomposition of *t*-BuOOH and the appearance of TMEO were followed simultaneously by GC under the same condition. The identity of the *t*-BuOOH eluent was established by GC–MS and also by the use of an authentic sample of *t*-BuOOH. In order to quantify the experimental peak areas, standard curves were prepared by using authentic *t*-BuOOH and TMEO. The concentration of each reactant was changed while holding the concentration of other reactants constant. In the absence of imidazole base (ligand) there is no reaction; neither the disappearance of *t*-BuOOH nor the appearance of TMEO was observed. The addition of imidazole results in the disappearance of *t*-BuOOH and also in the appearance of TMEO. Good pseudo-first-order kinetics is not seen when imidazole is less than threefold excess of (TPP)- $Mn^{III}Cl$. In all the experiments the following occurred: (i) the decomposition of *t*-BuOOH followed the first-order rate law in the absence of TME; (ii) in the presence of TME the decomposition of *t*-BuOOH is first-order at its higher concentrations, but at low concentrations the disappearance of the hydroperoxide is biphasic: an initial 15–20% fast component, followed by a slower reaction; (iii) the addition of TME decreased the rate of *t*-BuOOH disappearance; (iv) the addition of TME resulted in the first-order appearance of TMEO; and (v) in the presence of TME the observed pseudo-first-order rate constants for the disappearance of hydroperoxide (k_h) were found to be invariably greater by a factor of approximately two than the observed pseudo-first-order rate constants (k_e) for epoxide formation. The TME epoxidation reaction was also carried out with *N*-methylimidazole and *N*-(acetylphenyl)-imidazole. The yield of TME epoxide is only 9% for ligation by *N*-methylimidazole whereas the yield is ~35% for ligation by *N*-(acetylphenyl)imidazole, at $[(TPP)Mn^{III}Cl] = 6.2 \times 10^{-4}$ M, $[t-BuOOH] = 8.20 \times 10^{-3}$ M, TME = 0.1 M, and $[ligand] = 3.3 \times 10^{-3}$ M. The yield of TME epoxide with *N*-(acetylphenyl)imidazole is comparable with imidazole under identical concentrations of reactants. The reaction of *t*-BuOOH (6.0×10^{-3} M) with (TPP)- $Mn^{III}Cl$ (6.0×10^{-4} M) in the presence of pyridine (6.0×10^{-3} M) as ligand at TME = 0.4 M was found to be very slow. At approximately one $t_{1/2} = 7$ h, there was produced 4% of epoxide. These studies with pyridine, *N*-methylimidazole, and *N*-(acetylphenyl)imidazole as ligands were not pursued further.

Dependence upon Imidazole Concentration. At constant concentrations of (TPP)- $Mn^{III}Cl$ (6×10^{-4} M), *t*-BuOOH (8.2×10^{-3}

(7) Fieser, L. F.; Fieser, M. In *Reagents for Organic Synthesis*; John Wiley and Sons: New York, 1967; Vol. 1, p 136.

(8) Adler, A. D.; Longo, F. R.; Kampas, F.; Kim, J. J. *Inorg. Nucl. Chem.* **1970**, *32*, 2443.

(9) (a) Bruce, T. C.; Noar, J. B.; Ball, S. S.; Venkataram, U. V. *J. Am. Chem. Soc.* **1983**, *105*, 2452. (b) Johnson, R. M.; Siddiqui, I. W. In *The Determination of Organic Peroxides*; Pergamon Press: New York, 1970; pp 15–29.

(10) Traylor, T. G.; Lee, W. A.; Stynes, D. V. *Tetrahedron* **1984**, *40*, 553.

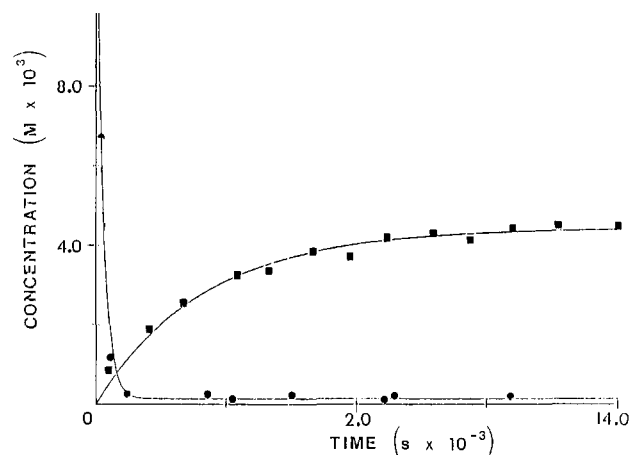


Figure 2. Plots of the disappearance (concentrations) of *t*-BuOOH (●) and appearance of the epoxide of TME (■) vs. time at $[\text{ImH}]_i = 9.0 \times 10^{-3} \text{ M}$, $[(\text{TPP})\text{Mn}^{\text{III}}\text{Cl}]_i = 6.0 \times 10^{-4} \text{ M}$, $[t\text{-BuOOH}]_i = 8.20 \times 10^{-3} \text{ M}$, and $[\text{TME}]_i = 0.40 \text{ M}$. Here the points are experimental, and the lines are generated from first-order rate equation.

M), and TME (0.4 M), both k_h and k_e increase with increase in the concentration of imidazole as given in Figure 1. It can be seen from Figure 1 that the rate constant for TMEO formation (k_e) first increases linearly with increase in $[\text{ImH}]_i$ and then approaches a limiting value at the highest imidazole concentration used (line A). At this low $[t\text{-BuOOH}]_i$, hydroperoxide disappearance is biphasic (loc. cit.). The time course for the disappearance of hydroperoxide could be fit to the appropriate equation for two sequential first-order processes. When the rate constants for the slow component and the rate constants for TMEO formation are plotted vs. $[\text{ImH}]_i$ (at $[\text{ImH}]_i \leq 4.0 \times 10^{-3} \text{ M}$), it is found that they fall on the same line (line A) whereas the rate constants for the fast component increase much more rapidly with increase in $[\text{ImH}]_i$ (Figure 1, line B). When $[\text{ImH}]_i \geq 9.0 \times 10^{-3} \text{ M}$, the rate of *t*-BuOOH disappearance was found to be too fast ($k_h = \sim 2.0 \times 10^{-2} \text{ s}^{-1}$) to follow whereas, under the same condition, the appearance of TMEO is slow, and it is conveniently measurable ($k_e = 1.08 \times 10^{-3} \text{ s}^{-1}$). These results establish that the oxidizing equivalents from *t*-BuOOH are converted into another oxidizing form which remains after the disappearance of *t*-BuOOH and serves as a source of oxygen atoms in the epoxidation process. This is dramatically pointed out in experiments with $[\text{ImH}] \geq 9.0 \times 10^{-3} \text{ M}$ where *t*-BuOOH disappearance is virtually complete but epoxide appearance has proceeded to but 10–20% completion of formation (Figure 2). At $[(\text{TPP})\text{Mn}^{\text{III}}\text{Cl}] = 6 \times 10^{-4} \text{ M}$, the yield of epoxide increases and then decreases with increase in $[\text{ImH}]$. The maximum yield of epoxide (~60%) was obtained when $[\text{ImH}]_i$ is in 15-fold excess over catalyst. The decrease in yield of epoxide at higher $[\text{ImH}]_i$ is presumably due to competition of ImH with both TME and *t*-BuOOH as an oxidizable substrate.

Dependence upon Manganese(III) Porphyrin Concentration.

The manganese(III) porphyrin concentration was varied in the range 1.2×10^{-4} – $6.0 \times 10^{-4} \text{ M}$ at constant $[\text{ImH}]_i = 3.0 \times 10^{-3} \text{ M}$, $[t\text{-BuOOH}]_i = 8.20 \times 10^{-3} \text{ M}$, and $[\text{TME}] = 0.40 \text{ M}$. The results are given in Figure 3. The rate constants for the formation of TMEO, k_e , as well as the rate constants for both the initial and rapid and the slower component for disappearance of *t*-BuOOH are linearly dependent upon the concentration of $(\text{TPP})\text{Mn}^{\text{III}}\text{Cl}$. This can be seen in the plots of Figure 3. Line A of the figure correlates the points for the appearance of epoxide and the final and slower rate of *t*-BuOOH disappearance while line B correlates the rate constants for the initial and rapid rates of *t*-BuOOH disappearance. Increasing $[(\text{TPP})\text{Mn}^{\text{III}}\text{Cl}]$ from 1.2×10^{-4} – $4.0 \times 10^{-4} \text{ M}$ with $[\text{ImH}]_i = 3.0 \times 10^{-3} \text{ M}$ and $[t\text{-BuOOH}] = 8.2 \times 10^{-3} \text{ M}$ provides epoxide in ~30% yield while $t_{1/2}$ changes from about 2.6 h to 55 min.

Dependence upon *t*-BuOOH Concentration. Holding the initial concentrations of $(\text{TPP})\text{Mn}^{\text{III}}\text{Cl}$ ($6.0 \times 10^{-4} \text{ M}$), ImH (3.0×10^{-3}

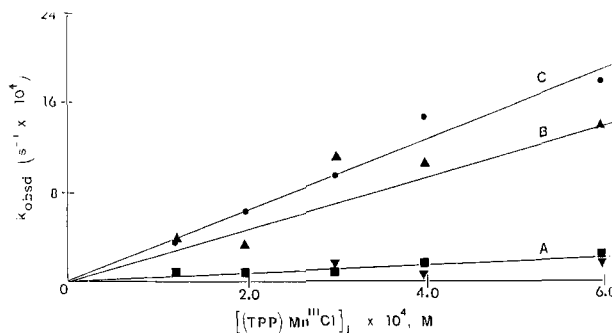


Figure 3. A plot of the pseudo-first-order rate constants (k_{obsd}) against $[(\text{TPP})\text{Mn}^{\text{III}}\text{Cl}]_i$ at constant $[t\text{-BuOOH}]_i = 8.20 \times 10^{-3} \text{ M}$, $[\text{ImH}]_i = 3.0 \times 10^{-3} \text{ M}$, and $[\text{TME}] = 0.40 \text{ M}$. Line A is the rate constant (k_e) for the formation of TMEO (■) and the rate constant of the slow component (k_h) for the decomposition of *t*-BuOOH (▼); line B is the rate constant (k_h) for the fast component of the decomposition of *t*-BuOOH (▲); and line C is the rate constant (k_h') for the decomposition of *t*-BuOOH in the absence of TME (●).

Table I. Effect of the Initial Concentration of *t*-BuOOH on the Rate Constant for *t*-BuOOH Disappearance (k_h) and Epoxide Appearance (k_e) at $[(\text{TPP})\text{Mn}^{\text{III}}\text{Cl}] = 6.0 \times 10^{-4} \text{ M}$, $[\text{ImH}] = 3.0 \times 10^{-3} \text{ M}$, and $[\text{TME}] = 0.40 \text{ M}$

$[t\text{-BuOOH}]_i, \text{ M}$	$k_h \times 10^4, \text{ s}^{-1}$	$k_e \times 10^4, \text{ s}^{-1}$
8.2×10^{-3}	4.76	2.18
2.47×10^{-2}	1.17	1.58
4.95×10^{-2}	2.31	1.51
8.20×10^{-2}	2.10	1.98
1.60×10^{-1}	1.63	2.30

Table II. Reaction of *t*-BuOOH ($8.20 \times 10^{-3} \text{ M}$) with Imidazole ($3.0 \times 10^{-3} \text{ M}$) Ligated Manganese(III) Porphyrin ($6.0 \times 10^{-4} \text{ M}$) in the Presence of TME. Effect of $[\text{TME}]$ on the Rate Constants k_h and k_e

$[\text{TME}]_i, \text{ M}$	$k_h \times 10^4, \text{ s}^{-1}$	$k_e \times 10^4, \text{ s}^{-1}$
0.02	4.48	1.85
0.06	3.86	1.15
0.10	3.60	1.72
0.40	4.76	2.18
0.70	4.38	4.05

M), and TME (0.40 M) constant, the initial concentration of *t*-BuOOH was varied between 8.20×10^{-3} and 0.165 M . The determined rate constants for hydroperoxide disappearance (k_h) and epoxide appearance (k_e) are given in Table I. Inspection of the table shows that both pseudo-first-order rate constants are independent of $[t\text{-BuOOH}]_i$ over a 20-fold change in its concentration. It should be noted that the turnover of the substrate by a catalyst, under the condition of nonsaturation of the catalyst with substrate, follows the first-order rate law and that the calculated pseudo-first-order rate constants are independent of the substrate concentrations, even though the initial rates are dependent upon the substrate concentrations. The finding that the values of k_e and k_h are independent of $[t\text{-BuOOH}]_i$ establishes that the reaction is first-order in *t*-BuOOH in this concentration range. However, at higher initial concentration of *t*-BuOOH, the disappearance of *t*-BuOOH does not go to 100% completion. The oxidation reaction may be initiated again by adding another aliquot of imidazole. This observation shows that imidazole is oxidatively consumed at higher concentrations of *t*-BuOOH.^{5b} The direct N-oxygenation of imidazole by *t*-BuOOH in the absence of $(\text{TPP})\text{Mn}^{\text{III}}\text{Cl}$ was followed by GC at $[\text{ImH}]_i = 6.0 \times 10^{-3} \text{ M}$ and $[t\text{-BuOOH}]_i = 6.0 \times 10^{-3} \text{ M}$. The change in $[t\text{-BuOOH}]$ amounted to only 10% in 7 h. This experiment shows that the direct reaction of *t*-BuOOH with ImH is negligible under our experimental conditions.

Dependence upon Olefin Concentration. With $[(\text{TPP})\text{Mn}^{\text{III}}\text{Cl}]_i = 6 \times 10^{-4} \text{ M}$, $[\text{ImH}]_i = 3 \times 10^{-3} \text{ M}$, and $[t\text{-BuOOH}]_i = 8.2 \times 10^{-3} \text{ M}$ the concentration of TME was varied between 0.02 and 0.70 M in order to determine the dependence of rate upon TME.

The results are shown in Table II. Table II shows that the rate constants k_h and k_e change by but twofold for this 35-fold change in TME concentration. Thus, epoxidation of TME by the manganese oxo species is not rate-determining in this system. It may be mentioned here that even though k_h and k_e are relatively constant, k_h is always greater than k_e by more than twofold. That disappearance of *t*-BuOOH always leads to the formation of epoxide suggests that the commitment step of oxygen transfer from *t*-BuOOH to manganese(III) porphyrin is followed by a slower step of alkene epoxidation or, alternatively, that the rate of oxygen transfer from *t*-BuOOH is slow and epoxidation of alkene is rapid but in competition with the oxidation of *t*-BuOOH. The latter explanation would appear to be correct. In the presence of TME, the rate of *t*-BuOOH consumption is slowed and the yield of the *t*-BuOOH oxidation product (*t*-BuO)₂ is decreased (vide infra).

The pseudo-first-order rate constant for the disappearance of *t*-BuOOH in the absence of TME (k_h') is greater than the pseudo-first-order rate constant for *t*-BuOOH disappearance (k_h) in the presence of TME. The rate constant k_h' shows linear dependence on [(TPP)Mn^{III}Cl], in the concentration range of 1.2×10^{-4} – 6×10^{-4} M (see Figure 3; line C). Similarly, k_h' increases with increase in the concentration of ImH in the range 1.0×10^{-3} – 4.0×10^{-3} M, as shown in Figure 1 (line C). The concentration of imidazole could not be increased to greater than 4.0×10^{-3} M, due to the inability to follow the faster reactions by the GC methodology used. Similarly, at higher [*t*-BuOOH]_i ($>1.0 \times 10^{-2}$ M) the reaction was too rapid to be followed by GC. With [(TPP)Mn^{III}Cl]_i = 1.2×10^{-4} – 6.0×10^{-4} M, [ImH]_i = 2.0×10^{-3} – 3.0×10^{-2} M, [*t*-BuOOH]_i = 8.2×10^{-3} M, and with [TME] = 0.40 M there is formed, in addition to TMEO (~35%), the species di-*tert*-butylperoxide ((*t*-BuO)₂) in approximately 1% yield whereas in the absence of TME the yield of (*t*-BuO)₂ is approximately 4%. The identity of the (*t*-BuO)₂ eluent was established by GC-MS spectrometry as well as by coinjection of an authentic sample of (*t*-BuO)₂.

Reaction in the Presence of 2,2-Diphenyl-1-picrylhydrazine (DPPH). The readily oxidizable DPPH (0.06 M) has been used by us in a previous investigation to trap higher valent manganese-oxo porphyrin species.⁶ With imidazole concentrations of 6.0×10^{-2} , 9.0×10^{-3} , and 3.0×10^{-3} M ([*t*-BuOOH]_i = 8.2×10^{-3} M and [(TPP)Mn^{III}Cl] = 6.0×10^{-4} M) the yields of epoxide (42%, 57% and 40%, respectively) with [TME]_i = 0.4 M were not influenced by the presence of DPPH. However, there is a decrease in the yields of the radical DPP•, due to the presence of TME. In the presence of DPPH and olefin there was obtained between 22%, 11%, and 7% of DPP• whereas in the absence of olefin 41%, 36%, and 13.5% of DPP• was formed. Thus, though *t*-BuOOH is consumed by oxidation of DPPH, the yield of epoxide is not reduced. These experiments can be explained with the assumption that TME is more reactive with intermediate (TPP)Mn^V(ImH)(O) than is DPPH. The pseudo-first-order rate constants for the formation of DPP• at [ImH]_i = 6.0×10^{-2} , 9.0×10^{-3} , and 3.0×10^{-3} M, keeping [*t*-BuOOH]_i at 8.2×10^{-3} M, [(TPP)Mn^{III}Cl]_i = 6.0×10^{-4} M, and [TME]_i = 0.4 M are 2.5×10^{-3} , 1.20×10^{-3} , and 4.1×10^{-4} s⁻¹, respectively. These values agree well with k_e obtained under similar conditions (see Figure 1). This observation suggests that both TMEO and DPP• are formed after the rate-determining step.

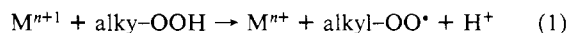
Discussion

The reactions and associated rate constants presented in Scheme I are kinetically competent for the reaction of *t*-BuOOH with (TPP)Mn^{III}Cl in the presence and absence of imidazole (ImH) and 2,3-dimethyl-2-butene (TME). The rate and equilibrium constants under the headings "(a) pre-equilibrium reactions" and "(b) rate-limiting oxygen transfer reactions" are known from a previous investigation from this laboratory⁶ (under the same experimental conditions as employed herein). These consist of the equilibrium constants for mono- and bis-ligation of ImH with (TPP)Mn^{III}Cl and the second-order rate constants for the reaction of the resultant (TPP)Mn^{III}(ImH)Cl and (TPP)Mn^{III}(ImH)₂ complexes with *t*-BuOOH. The rate constants k_1 , k_{-1} , k_2 , and

k_{-2} provide the correct experimental values for the pre-equilibrium constants $k_1/k_{-1} = K_1$ and $k_2/k_{-2} = K_2$. As such, the values of the rate constants may be increased, but the given ratios may not be varied. Thus, the kinetics for the rate-limiting and committing oxygen transfer from *t*-BuOOH to the imidazole ligated manganese(III) porphyrin species is known.⁶ After the rate-limiting oxygen transfer step, the reactive higher valent manganese(V)-oxo species (TPP)Mn^V(ImH)(O) transfers an oxene equivalent to TME to form TMEO, "(c) epoxidation reaction", and in this process (TPP)Mn^{III}(ImH) is regenerated. With this in hand there remains the proposal of a series of chemically plausible reaction steps, as given in Scheme I, which explains the various experimental observations which include the following: (i) Disappearance of *t*-BuOOH follows the first-order rate law in the absence of TME, while in the presence of TME, *t*-BuOOH disappearance follows two sequential first-order processes; (ii) formation of TMEO is cleanly first-order; (iii) the rate of disappearance of *t*-BuOOH is always more than twofold greater than that for epoxide appearance; (iv) the maximum yield of epoxide is but ~60%; (v) the % yield of epoxide increases and then decreases with increase in [ImH]_i; and (vi) there is formation of a small percentage of di-*tert*-butylperoxide, (*t*-BuO)₂.

In Scheme I, reactions which involve destruction of *t*-BuOOH and ImH by (TPP)Mn^V(ImH)(O) oxidations are included under the heading "(d) nonproductive oxidations". In the category "(e) oxygen transfer to imidazole" are included hypothetical reactions for the required formation of an alternate oxygen donor by transfer of an oxene equivalent to ImH. The rate constants for the non-rate-determining reactions of (c) and (d) as well as the partially rate-determining reactions of (e) were chosen by iteration in order to duplicate the experimental observations by computer simulation. The rate constants k_5 through k_{10} may all be increased at constant ratio, but they may not be decreased and as such represent minimal values. The rate constants for the reactions of (e) are set since k_{11} , k_{12} , and k_{13} pertain to reactions which at high [ImH]_i become rate-determining in epoxide formation.

The reactions "(d) nonproductive oxidations" have been included as a means of expending the oxygen equivalents of *t*-BuOOH without TME epoxidation (k_6 , k_7 , k_8 , and k_9) and the oxidation of imidazole ligand (k_{10}). The experimental observation that the pseudo-first-order rate constants for the decomposition of *t*-BuOOH are greater than the pseudo-first-order rate constants for epoxide formation by a factor of more than two suggests that there is an additional reaction for *t*-BuOOH consumption. By trials in computer-fitting with various reaction schemes, this must involve the reaction of *t*-BuOOH with the high valent manganese oxo species. It has not been previously observed, in the reaction of alkyl hydroperoxides with manganese(III) porphyrins, that the higher valent manganese(V) oxo porphyrin oxidizes the hydroperoxide species because the rates of epoxidation and hydroperoxide disappearance have not been compared in the same experiment. This is, however, a catalase type reaction, and there are numerous studies which establish that alkyl hydroperoxides are oxidized by higher valent metal ions.¹¹⁻¹³ In addition, it has been observed that the species (*t*-BuO)₂ is formed in nearly 2% of the [*t*-BuOOH]_i. Therefore, it is required to include the reactions of k_6 , k_7 , and k_8 in which the high valent manganese(V) species undergoes 1e⁻ reduction to form manganese(IV) oxo species and *t*-BuOO•. The proposed *t*-BuOOH reduction of the manganese(V) oxo species to a manganese(IV) oxo species is certainly plausible. It is generally accepted¹⁴ that the reaction of alkyl hydroperoxides with a metal ion in its high valent oxidation state occurs by 1e⁻ reduction of the metal oxidant and formation of the alkyl hydroperoxy radical (eq 1). It is also known that two



(11) Sheldon, R. A. *Recl. Trav. Chim. Pays-Bas* **1973**, *92*, 253.

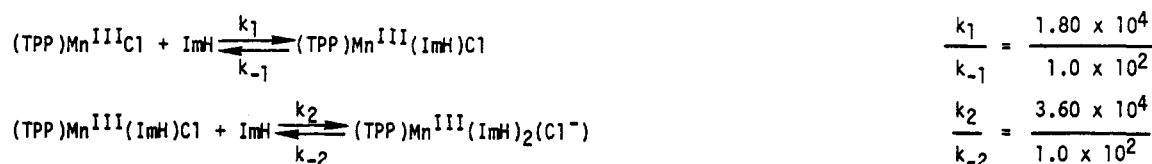
(12) Hiatt, R.; Irwin, K. C.; Gould, C. W. *J. Org. Chem.* **1968**, *33*, 1430.

(13) (a) Gould, E. S.; Hiatt, R. R.; Irwin, K. C. *J. Am. Chem. Soc.* **1968**, *90*, 4573. (b) Sharpless, K. B.; Verhoeven, T. R. *Aldrichimica Acta* **1979**, *12*, 63.

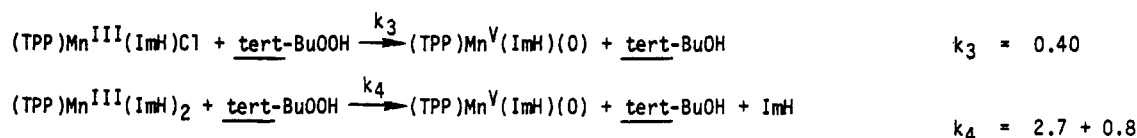
(14) Denisov, E. T.; Emanuel, N. M. *Usp. Khim.* **1960**, *29*, 1409.

Scheme I^a

(a) Pre-Equilibrium Reactions:



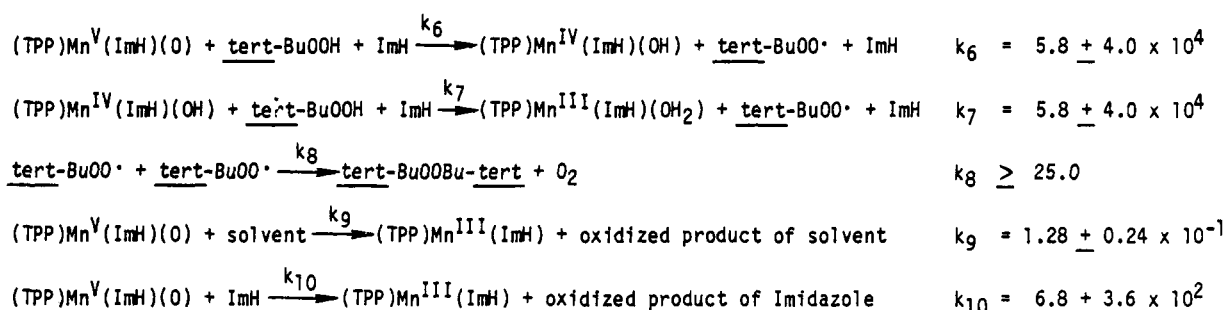
(b) Rate-Limiting Oxygen Transfer Reactions:



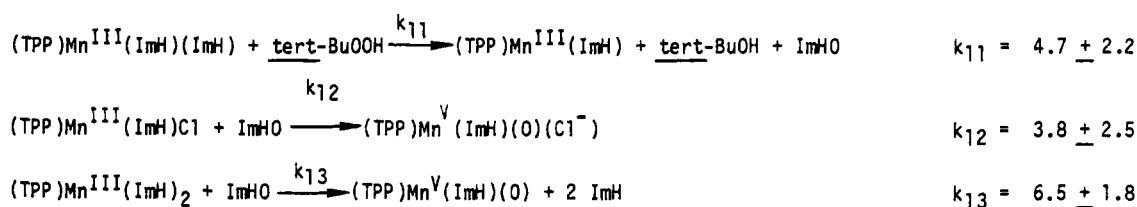
(c) Epoxidation Reaction:



(d) Non-Productive Oxidations:



(e) Oxygen Transfer to Imidazole

^aUnits: mols and s.

t-BuOO[•] react to form (*t*-BuO)₂ and O₂.¹⁵ It is required that the manganese-oxo porphyrin species which oxidize *t*-BuOOH (*k*₆ and *k*₇) are imidazole ligated and that the reaction is catalyzed by imidazole base (this requirement can be appreciated from the experimental observation that *t*-BuOOH is consumed rapidly at high [ImH] ≥ 9 × 10⁻³ M). The rate constants *k*₆, *k*₇, and *k*₈ were chosen by iteration so that their values account for the disappearance of *t*-BuOOH being twofold faster than formation of epoxide. In addition to the oxidation of *t*-BuOOH by the higher valent manganese-oxo species it is required that solvent is also oxidized. This assumption is necessary in order to account for the low yield of epoxide. The rate constant *k*₉ was determined by iteration to provide the correct yields of epoxide. Finally, the

oxidation of imidazole by manganese(V) oxo species was included so as to account for the observed oxidative consumption of imidazole at high [*t*-BuOOH]_i.

The necessity of including the reactions "(e) oxygen transfer to imidazole" is to explain the observation that at [ImH]_i ≥ 9.0 × 10⁻³ M disappearance of *t*-BuOOH is much more rapid than is the appearance of epoxide. Since there is not sufficient concentrations of manganese(III) porphyrin to store the oxidation equivalents required for the formation of the epoxide, these oxygen atoms must be stored for future use by being combined with another of the reactants. The only possibilities are that oxygen atoms are transferred to imidazole or to the solvent. Since the disparity between the rates of *t*-BuOOH consumption and epoxide formation increases with increasing imidazole concentration, it is reasonable to assume that there is the transient formation of an oxygenated imidazole species which acts like a second oxygen

(15) Sheldon, R. A.; Kochi, J. K. In *Metal Catalyzed Oxidations of Organic Compounds*; Academic Press: New York, 1981; Chapter 3, p 38.

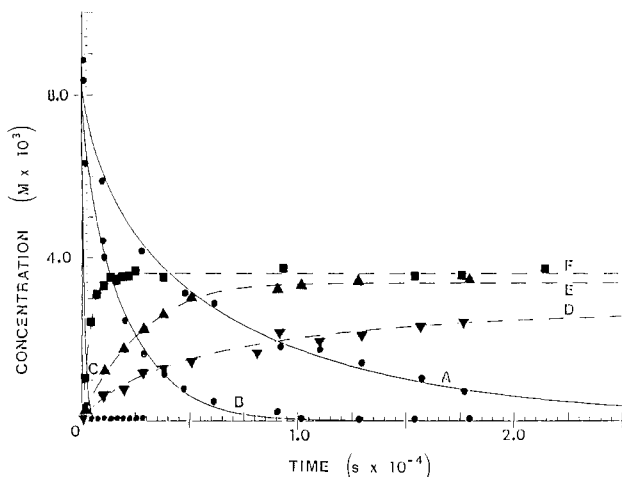
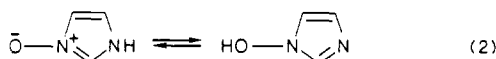


Figure 4. Representative fits of computer generated simulations (according to Scheme I and associated rate constants) for the disappearance of *t*-BuOOH and appearance of TMEO. The lines represent the simulations, and the points are experimentally determined. The following initial concentrations are constant at $[(\text{TPP})\text{Mn}^{\text{III}}\text{Cl}] = 6.0 \times 10^{-4} \text{ M}$, $[t\text{-BuOOH}] = 8.20 \times 10^{-3} \text{ M}$, and $[\text{TME}] = 0.40 \text{ M}$. In the experiments $[\text{ImH}]_i$ was allowed to vary. For the disappearance of *t*-BuOOH line A is for $[\text{ImH}]_i = 2.0 \times 10^{-3} \text{ M}$ (●); line B $[\text{ImH}]_i = 4.0 \times 10^{-3} \text{ M}$ (○); and line C $[\text{ImH}]_i = 6.0 \times 10^{-2} \text{ M}$ (▲). For the appearance of TMEO line D pertains to $[\text{ImH}]_i = 2.0 \times 10^{-3} \text{ M}$ (▼); line E $[\text{ImH}]_i = 4.0 \times 10^{-3} \text{ M}$ (△); and line F $[\text{ImH}]_i = 6.0 \times 10^{-2} \text{ M}$ (■).

transfer reagent. It is plausible that this species is the N-oxide of imidazole (eq 2). Attempts to prepare simple imidazole



N-oxides by reaction of imidazole with percarboxylic acids and alkyl hydroperoxides have not been fruitful, due to competing or following reactions which result in the disruption of the ring system.¹⁶ Thus, the oxidative destruction of imidazole derivatives by alkyl hydroperoxide has been proposed¹⁷ to be due to the initial formation of a radical intermediate by 4-addition of HO^\bullet to the imidazole ring. A similar reaction is most likely involved in the oxidative destruction of imidazoles by Fenton chemistry.¹⁸ However, 2,4,5-triphenylimidazole has been reported¹⁹ to be oxidized by perbenzoic acid to provide the corresponding N-oxide. The rate constant employed for oxygen transfer to imidazole from *t*-BuOOH (k_{11}) in the presence of imidazole ligated $(\text{TPP})\text{Mn}^{\text{III}}\text{Cl}$ species was arrived at by iteration. Also, the rate constants k_{12} and k_{13} for the subsequent reaction of imidazole N-oxide with mono- and bis-ligated manganese(III) porphyrin were determined by iteration. It should be noted that the rate constants k_{11} , k_{12} , and k_{13} were chosen in such a way that the epoxide formation follows the first-order rate law as it is observed experimentally. The direct N-oxygenation of imidazole by *t*-BuOOH in the absence of catalyst manganese(III) porphyrin is negligible.

Use of Scheme I with associated rate constants leads to a quantitative (within experimental error) correlation of the rates of disappearance of *t*-BuOOH and appearance of TMEO under the various experimental conditions (Figures 4, 5 and 6). In the experiments of Figure 4 the imidazole concentration was changed while the concentrations of $(\text{TPP})\text{Mn}^{\text{III}}\text{Cl}$, *t*-BuOOH, and TME were maintained constant. For the experiments of Figure 5, the concentration of $(\text{TPP})\text{Mn}^{\text{III}}\text{Cl}$ was changed, while the concentrations of ImH, TME, and *t*-BuOOH were held constant. And finally, in Figure 6 the concentration of *t*-BuOOH was changed,

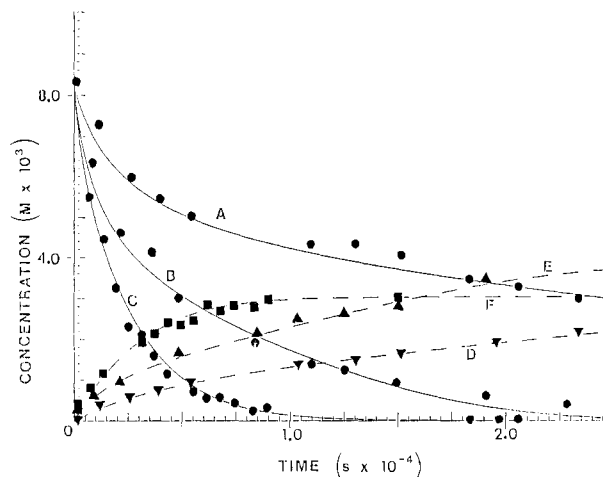


Figure 5. Representative fits of computer generated simulations (according to Scheme I with associated rate constants) for the disappearance of *t*-BuOOH and appearance of TMEO as a function of the concentration of $(\text{TPP})\text{Mn}^{\text{III}}\text{Cl}$. The lines represent the simulations, and the points are experimentally determined. The following initial concentrations are constant at $[t\text{-BuOOH}]_i = 8.20 \times 10^{-3} \text{ M}$, $[\text{ImH}]_i = 3.0 \times 10^{-3} \text{ M}$, and $[\text{TME}]_i = 0.40 \text{ M}$. Line A is disappearance of *t*-BuOOH at $[(\text{TPP})\text{Mn}^{\text{III}}\text{Cl}]_i = 1.20 \times 10^{-4} \text{ M}$ (●); line B $[(\text{TPP})\text{Mn}^{\text{III}}\text{Cl}]_i = 3.0 \times 10^{-4} \text{ M}$ (○); and line C $[(\text{TPP})\text{Mn}^{\text{III}}\text{Cl}]_i = 6.0 \times 10^{-4} \text{ M}$ (▲). Appearance of TMEO as a function of manganese(III) porphyrin concentration is as follows: line D is at $[(\text{TPP})\text{Mn}^{\text{III}}\text{Cl}]_i = 1.20 \times 10^{-4} \text{ M}$ (▼); line E at $[(\text{TPP})\text{Mn}^{\text{III}}\text{Cl}]_i = 3.0 \times 10^{-4} \text{ M}$ (△); and line F at $[(\text{TPP})\text{Mn}^{\text{III}}\text{Cl}]_i = 6.0 \times 10^{-4} \text{ M}$ (■).

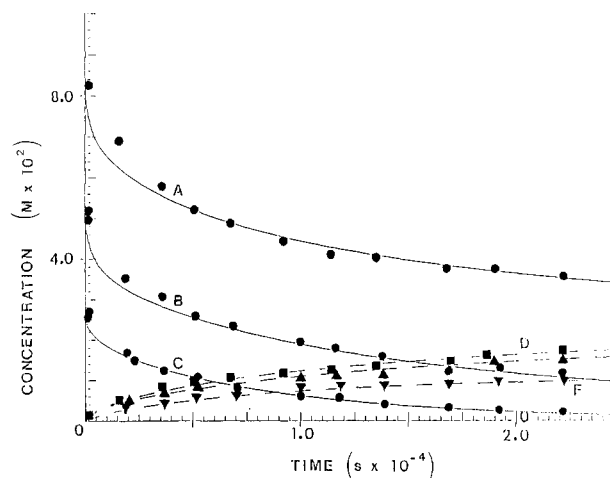


Figure 6. Representative fits of computer generated simulations (according to Scheme I and associated rate constants) for the disappearance of *t*-BuOOH and appearance of TMEO with time as a function of the $[t\text{-BuOOH}]_i$. The lines represent the simulations, and the points are experimentally determined at constant $[(\text{TPP})\text{Mn}^{\text{III}}\text{Cl}]_i = 6.0 \times 10^{-4} \text{ M}$, $[\text{ImH}]_i = 3.0 \times 10^{-3} \text{ M}$, and $[\text{TME}]_i = 0.40 \text{ M}$. Line A represents the disappearance of *t*-BuOOH at $[t\text{-BuOOH}]_i = 8.24 \times 10^{-2} \text{ M}$ (●); line B at $[t\text{-BuOOH}]_i = 4.95 \times 10^{-2} \text{ M}$ (○); and line C at $[t\text{-BuOOH}]_i = 2.47 \times 10^{-2} \text{ M}$ (▲). Line D is appearance of TMEO at $[t\text{-BuOOH}]_i = 8.42 \times 10^{-2} \text{ M}$ (▼); line E at $[t\text{-BuOOH}]_i = 4.95 \times 10^{-2} \text{ M}$ (△); and line F at $[t\text{-BuOOH}]_i = 2.47 \times 10^{-2} \text{ M}$ (■).

Table III. Effect of the Initial Concentration of 2,3-Dimethyl-2-butene (TME) on the Rate Constants k_h and k_e at $[(\text{TPP})\text{Mn}^{\text{III}}\text{Cl}]_i = 6.0 \times 10^{-4} \text{ M}$, $[t\text{-BuOOH}]_i = 8.20 \times 10^{-3} \text{ M}$, and $[\text{ImH}]_i = 3.0 \times 10^{-3} \text{ M}$

$[\text{TME}]_i, \text{ M}$	$10^4 \times k_h, \text{ s}^{-1}$		$10^4 \times k_e, \text{ s}^{-1}$	
	calcd	obsd	calcd	obsd
0.70	4.40	4.40	3.60	4.00
0.40	4.50	4.80	3.00	2.40
0.10	3.60	2.20	1.70	1.70
0.06	3.80	2.20	1.30	1.20

(16) (a) Botvinnik, M. M.; Porkofev, M. A. *J. Gen. Chem. U.S.S.R.* **1937**, 7, 1621. (b) Lettau, H. *Z. Chem.* **1970**, 10, 211.

(17) Yong, S. H.; Karel, M. *J. Food Science* **1979**, 44, 568.

(18) Imanaga, Y. *J. Biochemistry (Tokyo)* **1955**, 42, 669.

(19) Letourneux, G. C.; Lemaire, H.; Rassat, A. *Bull. Soc. Chim. Fr.* **1965**, 3283.

Table IV. Effect of the Initial Concentration of (TPP)Mn^{III}Cl on the Rate Constant (k_h') for the Decomposition of *t*-BuOOH (8.20×10^{-3} M) at [ImH]_i = 3.0×10^{-3} M in the Absence of TME

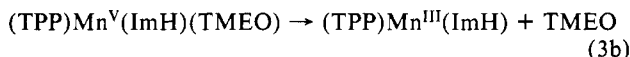
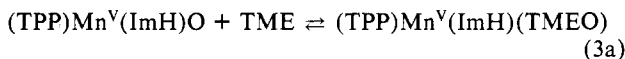
(TPP)Mn ^{III} Cl	$10^4 \times k_h', \text{s}^{-1}$	
	calcd	obsd
6.0×10^{-4}	14.0	17.5
3.0×10^{-4}	6.5	7.8
2.0×10^{-4}	4.6	4.3
6.0×10^{-4a}	22.2	24.6

^a [ImH]_i = 4.0×10^{-3} M.

keeping the concentrations of other reactants constant. The points of Figures 4, 5, and 6 are experimental, while the lines have been computer-generated from Scheme I and associated rate constants.

As a further means of judging the kinetic competence of Scheme I there is compared in Table III the calculated and observed rate constants for *t*-BuOOH disappearance (k_h) and epoxide formation (k_e) as a function of the initial concentration of alkene. In Table IV there is compared the observed and calculated rate constants for the disappearance of *t*-BuOOH in the absence of alkene (k_h') as a function of manganese(III) porphyrin catalyst concentration.

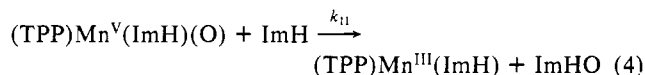
In Scheme I, the reactions of (a) "pre-equilibrium reactions", (b) "rate-limiting oxygen transfer reactions", and (c) "epoxidation reaction" had been determined explicitly in a previous study.⁶ The remaining reactions under the headings (d) and (e) have been arrived at as plausible only after the examination of many alternatives. An alternative explanation which was considered for the experimental observations that the rate of disappearance of the hydroperoxide is always greater than that for appearance of epoxide is that the transfer of oxygen from *t*-BuOOH to (TPP)Mn^{III}(ImH) and (TPP)Mn^{III}(ImH)₂ are committing steps but the epoxidation steps are rate-limiting. Computer simulation of this possibility was tested at [ImH]_i = 9×10^{-3} M, [(TPP)Mn^{III}Cl] = 6×10^{-4} M, [*t*-BuOOH]_i = 8.2×10^{-3} M, and [TME]_i = 0.4 M. At these concentrations it is observed that the rate of the hydroperoxide disappearance is markedly faster than that of epoxide appearance. The section (e) "oxygen transfer to imidazole" was omitted from Scheme I, and the section (c) "epoxidation reaction" was altered as shown in eq 3a and b. Here,



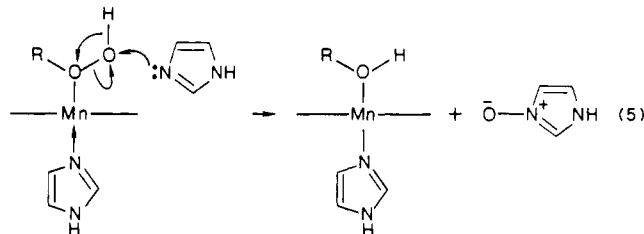
it is assumed that an intermediate is in equilibrium with the manganese oxo species and olefin and epoxide formation is rate-limiting. This alteration of Scheme I does not allow simulation of the experimental observation that the *t*-BuOOH is completely decomposed prior to the slow formation of epoxide. Also, under these conditions, if the complete disappearance of *t*-BuOOH is due to the accumulation of manganese(V) oxo species, one would anticipate a strong absorbance at about 420 nm characteristic of manganese porphyrins in the high valent oxidation states.^{4c,20-23} Spectral scanning with time of a reaction solution

([*t*-BuOOH] = 8.2×10^{-3} M, [(TPP)Mn^{III}Cl] = 6×10^{-4} M, [TME]_i = 0.4 M, and [ImH]_i = 9×10^{-3} M) did not reveal any significant increase in absorbance around 420 nm. In addition, repetitive spectral scanning with time in the absence of TME does not suggest the accumulation of an intermediate manganese(V) oxo species.

If one accepts the transfer of an oxygen from *t*-BuOOH to imidazole, two alternate mechanisms may be considered. These are (i) reaction of *t*-BuOOH with (TPP)Mn^{III}(ImH)₂ as used in Scheme I (k_{11}) and (ii) reaction of ImH with (TPP)Mn^V(ImH)(O) (eq 4). At low concentration of ImH ($\leq 4.0 \times 10^{-3}$



M), this latter possibility gives good computer fitting ($k_{11} = 1.0 \times 10^3 \text{ M}^{-1} \text{ s}^{-1}$) for the disappearance of the hydroperoxide as well as the formation of epoxide. At higher [ImH]_i (equal to 9.0×10^{-3} M or greater), however, the rapid rate of decomposition of *t*-BuOOH is not predicted by simulation, even when the rate constant k_{11} is significantly changed (over a range from 1.0×10^3 – 1.0×10^8). This is so, because under these conditions both the rate of decomposition of *t*-BuOOH and the rate of formation of epoxide are controlled by the initial rate-limiting reaction between *t*-BuOOH and the imidazole ligated species, (TPP)Mn^{III}(ImH)Cl and (TPP)Mn^{III}(ImH)₂. This shows that the high valent manganese oxo species does not oxygenate imidazole to form the alternate oxygen transfer reagent at high [ImH]. The foregoing arguments, along with the computer-fitting results, clearly indicate the kinetic competence of the imidazole ligand being oxygenated by reaction of *t*-BuOOH with (TPP)Mn^{III}(ImH)₂. The most likely path by which such an oxygen transfer to imidazole could occur is given in (eq 5).



Collman and co-workers⁴ using hypochlorite as the oxygen transfer agent and a solvent biphasic of H₂O/toluene with phase transfer catalyst have provided results in support of alkene dependency in the rate-limiting step. They have postulated the formation of a metallaoxetane intermediate whose breakdown is the rate-determining step of the catalytic cycle. If such an intermediate were to be formed in the present system, it would arise after the rate-limiting transfer of oxygen from *t*-BuOOH to manganese(III) porphyrin. Our observations are not contradictory of those from Collman's laboratory. Oxygen transfer from hypochlorite is likely to be much more facile than is oxygen transfer from *t*-BuOOH, because Cl⁻ is a better leaving group than is *t*-BuO⁻, and, of course, the solvent systems employed are quite different.

Acknowledgment. This work was supported by a grant from the National Institutes of Health.

(20) (a) Carnieri, N.; Harriman, A.; Porter, G. *J. Chem. Soc., Dalton Trans.* **1982**, 931. (b) Carnieri, N.; Harriman, A.; Porter, G.; Kalyanasundaram, K. *J. Chem. Soc., Dalton Trans.* **1982**, 1231.

(21) (a) Hill, C. L.; Schardt, B. C. *J. Am. Chem. Soc.* **1980**, *102*, 6374. (b) Camenzind, M. J.; Hollander, F. J.; Hill, C. L. *Inorg. Chem.* **1982**, *21*, 4301. (c) Smegal, J. A.; Schardt, B. C.; Hill, C. L. *J. Am. Chem. Soc.* **1983**, *105*, 3510. (d) Camenzind, M. J.; Hollander, F. J.; Hill, C. L. *Inorg. Chem.* **1983**, *22*, 3776.

(22) (a) Groves, J. T.; Kruper, W. J., Jr.; Haushalter, R. C. *J. Am. Chem. Soc.* **1980**, *102*, 6375. (b) Groves, J. T.; Watanabe, Y.; McMurtry, T. J. *J. Am. Chem. Soc.* **1983**, *105*, 4489.

(23) Bortolini, O.; Meunier, B. *J. Chem. Soc., Chem. Commun.* **1983**, 1364.